actuators

MDPI

Article

Design and Testing of Accurate Dicing Control System for Fruits and Vegetables

Song Mei [1], Fengque Pei [2], Zhiyu Song [1,*] and Yifei Tong [3]

[1] Nanjing Institute of Agricultural Mechanization, Ministry of Agriculture and Rural Affairs, Nanjing 210014, China
[2] College of Mechanical and Electrical Engineering, Hohai University, Changzhou 213022, China
[3] School of Mechanical Engineering, Nanjing University of Science and Technology, Nanjing 210094, China
* Correspondence: songzhiyu@caas.cn

Abstract: It is hard to control the dicing size of current fresh-cutting devices for fruits and vegetables precisely, and this can be influenced by complex working environments. This paper looks at traditional three-dimensional fresh-cutting machines and, apart from analyzing the force-and-motion equation to determine the minimum rotational speed of the roller, the cross-cutting tool's independent drive system, the speed detection system of the material before dicing, and shaft-speed monitoring have also been analyzed in order to develop precise control technology for three-dimensional fruit and vegetable dicing by considering dicing input-speed detection and by fine-tuning the cross-cutting tool's dicing speed. Performance tests are carried out on the prototype before and after improvement. The results show that when the size of carrots and potatoes was 11 mm × 10 mm × 10 mm and 11 mm × 10 mm × 12 mm, the slice thickness and strip thickness error before improvement were 20% and 5%, respectively. Due to the structural limitations, the slice error was large, but the strip error as ideal. The dicing error was greater than 15% due to the different damping coefficients of the materials and the variable speed movement. After the adjustment, the overall dicing error was less than 10%, and the accuracy and stability were higher.

Keywords: fruits and vegetables; dicing; strip cutting; slicing; error

Citation: Mei, S.; Pei, F.; Song, Z.; Tong, Y. Design and Testing of Accurate Dicing Control System for Fruits and Vegetables. *Actuators* **2022**, *11*, 252. https://doi.org/10.3390/act11090252

Academic Editor: Paolo Mercorelli

Received: 10 August 2022
Accepted: 28 August 2022
Published: 1 September 2022

1. Introduction

The fresh cutting of fruits and vegetables, which mainly includes slicing, strip cutting, and dicing, is an important part of fresh product production in the current fruit and vegetable production chain. With the development of urbanization, people are now moving towards efficient and fast-paced household lifestyles. An increasing need for fresh-cut fruits and vegetables is seen among residents, so the supply of them has been rising in markets, takeaway food outlets, and in logistics. At the same time, major catering enterprises need more fresh-cut fruits and vegetables to save time. Moreover, consumers are also picky about the shape of fresh-cut fruits and vegetables, as messy and irregular fruits or vegetables are less appealing. Therefore, high-precision fruit- and vegetable-cutting machinery is urgently needed to meet current market demand [1,2].

In the process of the modern manufacturing industry's progress from industry 4.0 to 5.0, people are now exploring technology for machine control and intelligence, trying to apply it to industries [3,4]. Filipescu A et al. [5] proposed a communication and control architecture with a flexible assembly and a maintenance-integrated production line based on complex autonomous systems. Morgan J et al. [6] reviewed the basic research on these topics; on the problems and challenges of reconfigurable systems (RMS); and on the related technologies and prospects of machine control and machine intelligence. Morgan's research showed readers the ability of next-generation industry 4.0 machines to demonstrate intelligence and reconfigurability. Massaro A et al. [7] designed an intelligent control and drive system of

adaptive industry 5.0 equipment for the railway industry and designed three new maintenance and test protocols, respectively. Agricultural machinery and equipment also need to be improved to meet the increasing demand for automated agricultural machinery. In terms of the slicing, strip cutting, and dicing of fruits and vegetables, mechanized cutting has completely replaced manual work. Research has been conducted on related machines that can meet the above three requirements. Their processing modes can commonly be divided into continuous feeding, slicing, strip-cutting, and dicing steps, different combinations of which can satisfy multiple fruit- and vegetable-processing requirements and can improve the efficiency and quality of processing. The working modes of the machines mentioned above can be divided into plane-conveying sequential cutting and three-dimensional specification cutting. The former requires fruits and vegetables to be clamped, which affects the production efficiency, while the latter uses centrifugal slicing technology with disc cutting and cross cutting, which can greatly improve the processing efficiency. Currently, the main machines on the international market include the G-A fruit and vegetable dicing machine developed by Urschel in the USA, the McS-3d 3D vegetable dicing machine produced by FAM in Belgium, and the U3A dicing machine developed by Japan [8–11]. Chinese machines, such as the LG-350 and the LG-400 dicing machines developed by Jiangsu Ligong Fruit and Vegetable Machinery Co. Ltd., see relatively higher error rates during slicing and dicing when the processed section is over 10 mm due to insufficient study of the dicing and the cutting control mechanisms [12–16]. Heqi Jin et al. [17] used virtual prototype technology to solve the problems of large arc and the tilt of the dicing section in three-dimensional dicing machines for fruits and vegetables. The curve equation of the material-cutting section was carefully analyzed to improve the regularity of the cutting shape. The results showed that neatly diced section shapes with small-section deviations of three sizes were cut out, among which, the maximum percentage of the section's relative deviation was 12.7%. Jian-ping Hu [18] from Jiangsu University combined the three-dimensional fresh-cutting machine produced by Ligong Machinery for preliminary studies on the dicing mechanism, providing a theoretical basis for the improvement of its precision. However, through experimental comparison and analysis, the precision of dicing is still unstable, the main reason for which is the stress difference caused by the variable working environment, the differences in the water content of the cut materials, and the unequal distribution of internal components, affecting the stability of the output speed of the material being strip cut. This paper will further this research by integrating a dicing mechanism and dicing precision control system into the conducted research to improve the dicing precision of the machine.

In Section 2.1, the three-dimensional mechanism for the dicing of fruits and vegetables is analyzed. First, the mathematical model of centrifugal slicing is built, and the design parameters of the minimum rotational speed are extracted. Then, a three-dimensional mathematical model of dicing is built according to the relationship between controlling the cutting frequency and size, and the key output speed parameters for strip cutting that affect the dicing accuracy are extracted. In Section 2.2, a high-precision dicing detection and control system is developed based on the output speed detection of the cutting material and the independent control of the cutting tool's frequency. In Section 3, a speed detection system is used to carry out comparative tests by controlling different materials. Finally, the results are discussed, and the conclusions are summarized.

2. Materials and Methods

2.1. Mechanism Analysis of Dicing Fruits and Vegetables

2.1.1. Main Structure and Working Principle of Fruit and Vegetable Dicing Machines

Based on the LG-400 dicing machine developed by Jiangsu Ligong Fruit and Vegetable Machinery, this paper analyzes the machine's structural features and working principle. The dicing machine is composed of a slicing tool and roller assembly, a strip-cutting assembly, and a dicing assembly. The driving parts of the roller, strip-cutting tool, and

dicing tool are isolated by sealing structure, the working area of which generates no gas, liquid, or other pollution, making the machine structure compact.

When the machine is working, fruits and vegetables are placed into the roller, while the motor drives the roller rotation, causing the propeller to rotate the fruits and vegetables at a high speed and pushing the fruits and vegetables to the fixed location of the slicing tool to undergo slicing. Sliced fruits and vegetables enter the strip-cutting interface at a certain speed and are strip cut by a combination of the strip-cutting tool, gravity, and the corresponding friction. Finally, the strip-cut fruits and vegetables are diced in the discharge hole by the dicing tool. The cutting speed ratio is calculated according to the design of the three-dimensional cutting size requirements.

2.1.2. Design of Minimum Rotational Speed for Fruits and Vegetables Cut by Centrifugal Force

In the process of fruit and vegetable slicing, apart from ensuring the cutting force of the tool, fruits and vegetables should be close to the inner shell of the roller to prevent the fruits and vegetables from jumping, affecting the precision of the slicing. The centrifugal cutting force of fruits and vegetables [19,20] is expressed in Figure 1.

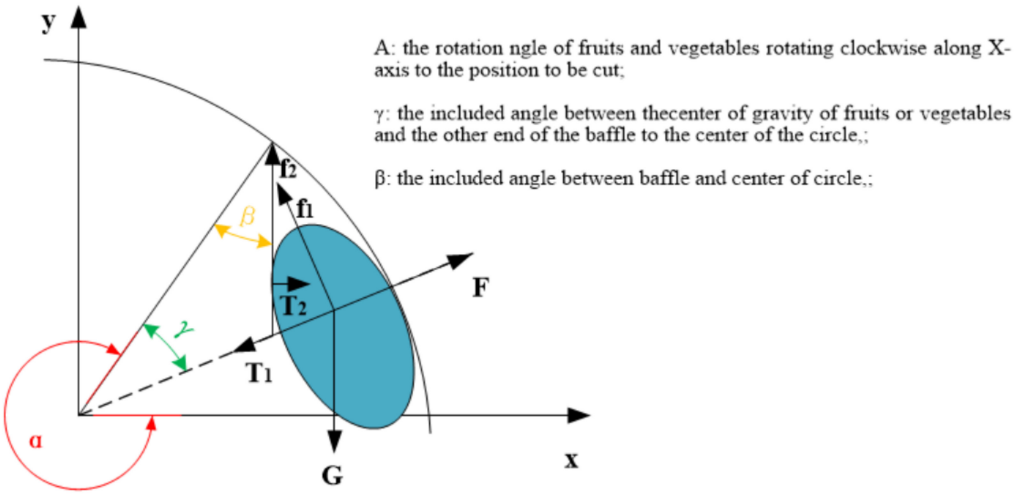

Figure 1. Cutting force diagram of fruits and vegetables cut by centrifugal force.

According to the force analysis at the cutting position in Figure 1, the dynamic balance equation without cutting force is:

$$\begin{cases} G\cdot\sin(2\pi-\alpha-\gamma)+T_1=T_2\cdot\sin(\beta+\gamma)+F+u_s\cdot T_2\cdot\cos(\beta+\gamma) \\ G\cdot\cos(\alpha+\gamma)+T_2\cdot\cos(\beta+\gamma)=u_d\cdot T_1+u_s\cdot T_2\cdot\sin(\beta+\gamma) \end{cases} \quad (1)$$

where G is the fruit and vegetable dead weight, N; T_1 is the tangential force exerted by the inner wall of the roller on the fruits and vegetables, N; T_2 is the normal baffle force on the fruits and vegetables, N; f_1 is the friction force on the contact surface between the fruits and vegetables and the inner wall of the roller, N; f_2 is the friction force between the fruits and vegetables and the baffle, N; F is the centrifugal force on the fruits and vegetables, N; α is the rotation angle of the fruits and vegetables rotating clockwise along the X-axis to the position to be cut, rad; β is the included angle between the baffle and the center of the circle, rad; γ is the included angle between the center of gravity of the fruits or vegetables and the other end of the baffle to the center of the circle, rad; u_s is the static friction coefficient between the fruits and vegetables and the baffle; and u_d is the dynamic friction coefficient between the fruits or vegetables and the inner wall of the roller. It can be derived from Equation (1) that

$$F=-G\cdot\sin(\alpha+\gamma)+T_1-\frac{[u_d\cdot T_1-G\cdot\cos(\alpha+\gamma)]\cdot[\sin(\beta+\gamma)+u_s\cdot\cos(\beta+\gamma)]}{\cos(\beta+\gamma)-u_s\cdot\sin(\beta+\gamma)} \quad (2)$$

where T_1 is the resultant balance force exerted by the fruits and vegetables, and F is the centrifugal force exerted by the fruits and vegetables, which is calculated as follows:

$$F = M = m \cdot \omega_1^2 \cdot \left(R_1 - \frac{D}{2} \right) \tag{3}$$

As shown in Equation (2), when $T_1 \geq 0$, the fruits and vegetables will cling to the wall of the roller. With the change in the rotation angle, when $T_1 = 0$, the corresponding critical value of ω_1 is different. Therefore, when one circle is rotating, the critical minimum rotational speed set at each position can be found. By choosing one of the largest values from the set, the minimum angular speed ω_{1min} satisfying the design requirements can be found. The minimum speed expression is as follows:

$$\omega_{1min} = \sqrt{\frac{\tan(\beta + \gamma) + u_s}{1 - u_s \cdot \tan(\beta + \gamma)} \cdot \frac{g \cdot \cos(\alpha + \gamma)}{R_1 - D/2} - \frac{g \cdot \sin(\alpha + \gamma)}{R_1 - D/2}} \tag{4}$$

The minimum rotational speed n_{1min} is as follows:

$$n_{1min} = \frac{60}{2\pi} \cdot \sqrt{\frac{\tan(\beta + \gamma) + u_s}{1 - u_s \cdot \tan(\beta + \gamma)} \cdot \frac{g \cdot \cos(\alpha + \gamma)}{R_1 - D/2} - \frac{g \cdot \sin(\alpha + \gamma)}{R_1 - D/2}} \tag{5}$$

where $\beta, \gamma, R_1, \textit{and } D$ are the fixed design values, and u_s is the friction coefficient being tested. The speed changes with the variable α. In this paper, the maximum value $n_{1max} = \max(n_{1min}(\alpha))(0 \leq \alpha \leq 2\pi)$ is selected as the lower limit of the design.

Matlab was used to simulate and solve the curves, as shown in Figure 2.

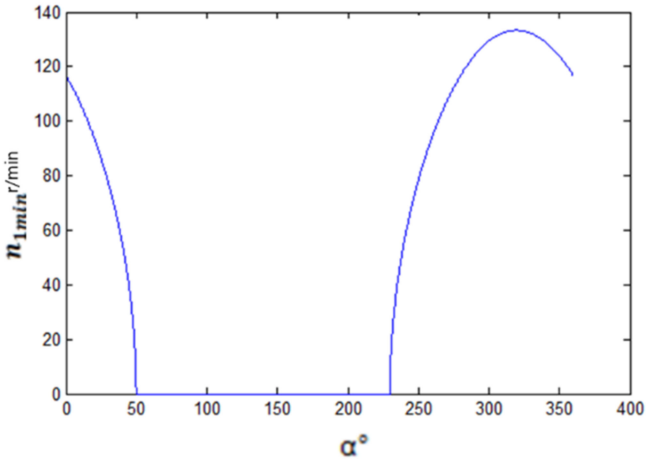

Figure 2. Simulation diagram of minimum rotational speed.

According to the value of the lowest angular speed, the highest position n of the minimum rotational speed curve can be solved as follows:

$$n_{max(1min)} = \max(n_{1min}) = 133 \text{ rpm} \tag{6}$$

2.1.3. Stress and Motion Analysis of Sliced Fruits and Vegetables

After fruits and vegetables have been cut by slicing tools, the sliced material will enter the downward transport mechanism and will arrive at the working area of the strip-cutting tool via the effects of gravity and friction. Then, after being strip cut, the material is subjected to the downward slope friction, which gradually increases and then decreases with changes in the contact area. Until the material is completely strip cut, the speed of the sliced material is invariable under the combination of the variable friction of the slicing tool, the invariable gravity, and the slope friction of different friction coefficients

(the water content and the distribution of components are different). Changes in this speed can be significantly influenced by the environment (humidity, temperature, material water content, and material fiber or starch, etc.), which cannot be calculated precisely. However, it is certain that the output speed of the strip material and the initial speed of the sliced material entering the slope is different. According to this feature, this research intends to design a material-conveying speed detection system to estimate the average output speed of strip materials, providing an optimal equation for dicing section shape with important parameters, guiding the precise operation of the cross-cutting tool, and improving dicing precision.

2.1.4. The Analysis of Section Shapes and Parameters of Dicing

In Jian-ping Hu's study [8], when fruits and vegetables move along the strip-cutting tool and the slicing output channel, assuming that fruits and vegetables move downward at a uniform speed and that the increased discharge distance per unit time is Δs, as the factor of increasing speed caused by friction is not taken into account, the dicing size is always larger than the preset size, and the exceeding error is relatively large. In this paper, the speed of the added strip materials increases, which is caused by friction. As such, a fine-tuned model of the relative speed between the dicing tool and the strip-cutting tool is obtained, which is shown below.

As shown in Figure 3, the material moves downwards along the slicing tool. It moves at a variable speed through the friction cutting mechanism via the disc tool. The nose of the dicing tool cuts the material at point A. When the tool nose turns at angle ∅ towards point B through the tool shaft, point E in the material moves downwards at the distance of EB along the slicing tool. In the same way, when the nose of the dicing tool turns to point C, the corresponding point F in the material moves downwards at the distance of FC. Therefore, the curve AEF is the shape of the cutting line of the dicing section. The coordinate system in the figure above is constructed with the center of the dicing tool's axis as the origin. The equation for the dicing section's AEF is as follows:

$$\begin{cases} x = d - h - \overline{AB}\sin\left(\frac{\pi-\varphi}{2} - \beta\right) \\ y = R_3\cos\beta - \overline{AB}\cos\left(\frac{\pi-\varphi}{2} - \beta\right) + v_2 \cdot \frac{\varphi}{\omega_3} \\ v_2 = (\omega_1 + \Delta\omega)\cdot R_1 \end{cases} \tag{7}$$

where h is the vertical distance from the center of the dicing tool to the back of the slicing tool, mm; d is the thickness of the sliced material, mm; R_3 is the radius of gyration of the dicing tool's nose, mm; φ is the angle that the dicing tool turns towards when cutting the material, rad; β is the angle between line AO and line AM, rad; $v_2 = (\omega_1 + \Delta\omega)\cdot R_1$ is the average speed detected by two pairs of photoelectric sensors after the material is cut, which is close to the real output speed, m/s; the angle between line AO and AM is $\beta = \arcsin\left(\frac{h-d}{R_3}\right)$; and the chord length is $\overline{AB} = 2R_3\sin\frac{\varphi}{2}$.

According to the literature [8], the main factors that influence the dicing section's shape are the rotational speed of the centrifugal cutting roller ω_1 and the rotational speed of the dicing tool ω_3. In this paper, the material moves at a variable speed during the strip-cutting process. The rotational speed ω_2 can accelerate or decelerate the material. Therefore, this paper intends to take the value of $\frac{\omega_1}{\omega_2}$ from Hu's study as a reference, while the detected average speed of the discharged strip materials is v_2. Plane-coordinate fitting is carried out in Equation (1) to obtain the optimal symmetrical dicing arc surface, and finally, ω_3 is adjusted.

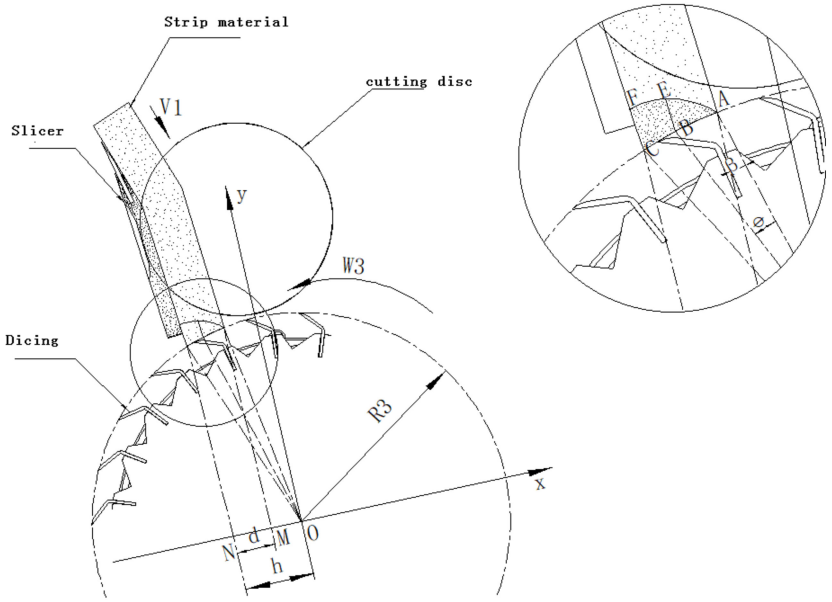

Figure 3. Diagram of dicing to shape.

2.2. Design of Three-Dimensional High-Precision Dicing Control System

2.2.1. Improved Design Scheme of Three-Dimensional Dicing Machine

The improved design scheme of this machine can mainly be divided into two parts: the first part is the main components, including the combination of the slicing, strip-cutting, and dicing tools, feeding the silo and frame, and the other part is the electrical control system for the tool speed and the tool rotation. Among them, the slicing and strip-cutting components share one power supply that is equipped with one control system, and the dicing component is equipped with a separate control system.

Firstly, the design requirements are as follows:

- Suitable for slicing, strip cutting, and dicing all kinds of fresh fruits and vegetables.
- Cutting size: slices of 10–20 mm, strips of 10–20 mm, diced segments of 10–20 mm.
- Production capacity: 1000–4000 kg/h.

The design for the whole machine is described below.

It can be seen from Figure 4 that fruits or vegetables first enter the feed inlet, and then, the propeller rotates, so the fruits and vegetables are loaded into the slicing component. Then, the sliced fruits and vegetables enter the disc tool's operation area and are cut into strips. After that, the strips of fruits and vegetables fall into the cross-cutting tool's operation area, are diced according to the tool size, and, finally, are discharged through the discharge port.

The rotary dicing device is driven by a three-phase AC variable-frequency asynchronous motor. A material sensor is installed before and after the discharge channel, and the output end of the material sensor is connected to the controlled end of the three-phase AC variable-frequency asynchronous motor through the control circuit. In this way, the control circuit can easily obtain the output speed of the material, which is cut into strips according to the signal difference between the front and rear material sensors, and can control the rotational speed of the rotary dicing device according to the corresponding setting requirements to realize precise size control during dicing in a closed-loop control mode.

It can be seen from Figure 5 that transmission sensor 1 is matched with receiver 1 and that transmission sensor 2 is matched with receiver 2. The two sets of sensors are located between the adjacent disc cutting tools and on the lower side. The two sets of sensors are distributed along the direction of the material at certain intervals. The speed can be calculated and analyzed based on the differences between the two groups of sensing signals.

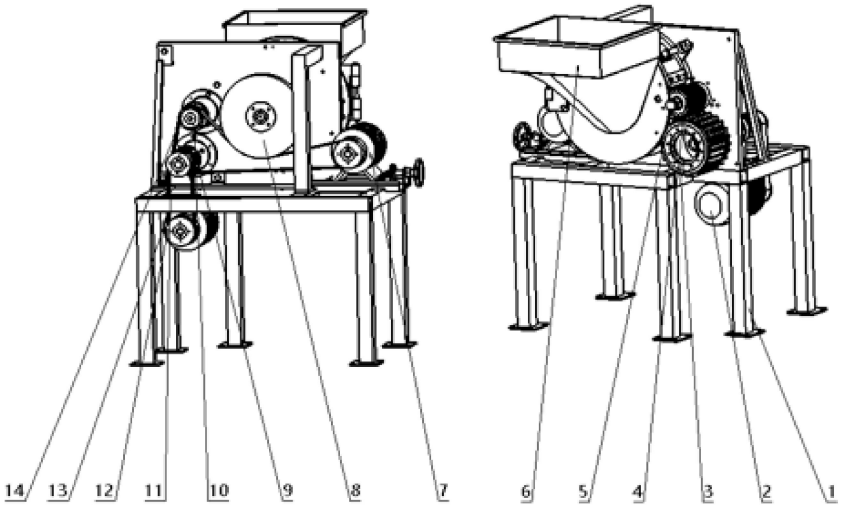

Figure 4. Diagram of the whole machine design. 1. Frame; 2. motor 2; 3. cross-cutting tool assembly; 4. disc tool assembly; 5. slicing outlet; 6. propeller shell and valve assembly; 7. motor 1; 8. propeller drive assembly; 9. tension wheel; 10. disc tool drive assembly; 11. cross-cutting drive assembly; 12. motor 2 output wheels; 13. L-type double-sided toothed synchronous belt 1; 14. L-type double-sided toothed synchronous belt 2.

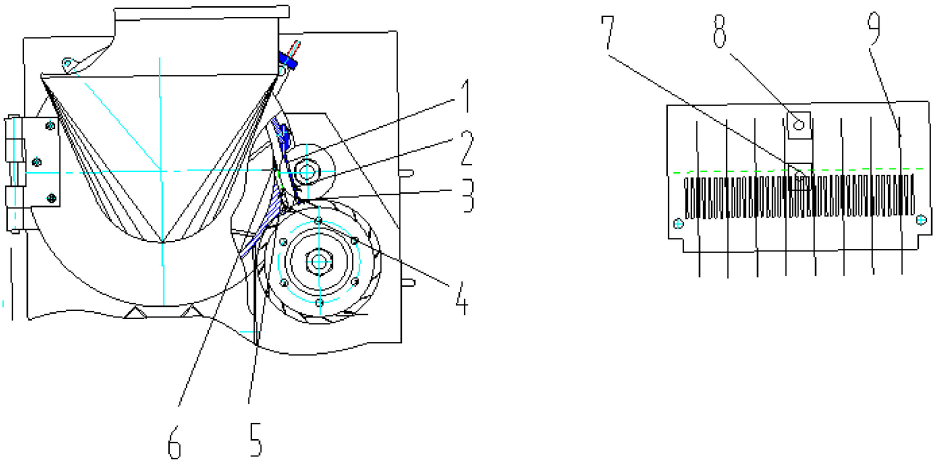

Figure 5. Diagram of speed sensor layout. 1. Upper guide plate; 2. receiver 1; 3. receiver 2; 4. transmission sensor 2; 5. transmission sensor 1; 6. slicing tool; 7. transmission sensor 1 position; 8. transmission sensor 2 position; 9. disc cutting tools distributed at various intervals.

Finally, the calculation principle of the real-time change in the driving parameters of the cross-cutting tool is as follows:

In this machine, motor 1 works at 2.2 kW and is driven by a gear belt. According to the transmission ratio, the propeller's transmission wheel and the disc cutting tool's transmission wheel are driven. Motor 2, which works at 0.75 kW, is selected to drive the cross-cutting tool's transmission wheel through a synchronous belt.

In this machine, motors 1 and 2 output synchronous wheels with 32 teeth. The diameter of the propeller is 400 mm and has a synchronous wheel of 112 teeth. The diameter of the disc cutting tool is 100 mm, and the synchronous wheel has 28 teeth. The diameter of the cross-cutting tool is 220 mm, and the synchronous wheel has 27 teeth. According to the transmission mode before the modification of the plan, motor 1 drives the propeller and the disc tool. When motor 1 rotates at 680 rpm, the propeller rotates at 194 rpm, and the disc tool rotates at 777 rpm. According to the settings before the modification of the plan, the cross-cutting tool speed is 806 r/min and is output by motor 2, which has asynchronous wheel with 32 teeth, so the output speed of motor 2 can be preset at

806 r/min. In the following section, we will modify the output speed of motor 2 based on the actual detection speed.

2.2.2. Strip-Cutting Output Speed Detection and Dicing Speed for Fine-Tuning System Design

Firstly, the schematic design of the speed detection and dicing speed fine-tuning system is presented below.

This paper takes PLC as the field data processing equipment for the processor, and designs the circuit which matches the control in detail, including the power supply, alarm, sensor, interface converter, etc. as shown in Figure 6.

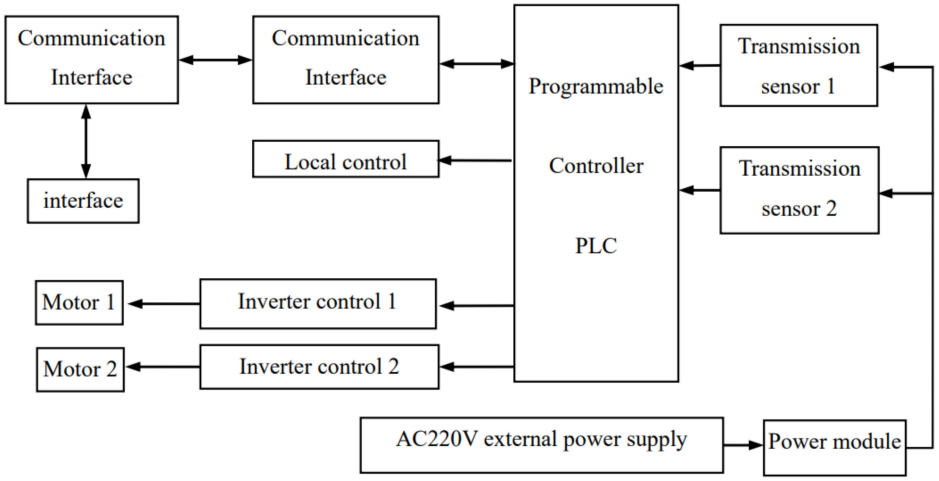

Figure 6. Diagram of slave machine hardware.

As shown in Figure 6, the slave hardware adds two sets of transmission photoelectric sensors with a fixed distance s to realize the average speed detection of the material displacement of s distance. In order to ensure that the detection is not disturbed, the installation distance s of the two sets of sensors is required to be less than the minimum distance of strip material. The calculation logic is shown in Figure 6.

The selection of the specific components of the slave machine needs to be further screened, and the hardware performance should be examined in combination with actual needs. The hardware selection is as follows: PLC selects Mitsubishi FX2N-48MR-001, 24 points input, 24 points output, which meets the system requirements, and FX2N-48MR-001 comes with a transformer, which should be connected to an external 50 Hz, 220 V AC power supply; the power supply module uses DC24V to supply power to the sensor, and the model is SZCK-623-1; the communication interface chip selects RS484S_CTM8251T that matches the 485 trunk The output mode is asynchronous half-duplex differential output, the transmission rate is faster, 300~115.2 KBPS; the transmission sensor 1, 2, namely the transmission type photoelectric sensor, choose CX-412A-C05. The power supply voltage of the two sets of sensors is DC24V. Motor 1 selects YE3-112M-6, a three-phase AC asynchronous motor controlled by a 2.2 KW inverter, with a rated speed of 935 r/min. Motor 2 selects YE2-80M2-4, a three-phase AC asynchronous motor controlled by a 0.75 KW inverter, with a rated speed of 1390 r/min. The interface design of the upper computer adopts XinJie TG765-MT touch screen.

The system's software design is as follows:

According to the system requirements, a flow chart of the main program of the slave machine is shown in Figure 7. As is shown in Figure 7, the main program of the slave machine is mainly composed of the slave machine itself and the sensors' data communication subroutine, timing subroutine, speed detection and inverter 2 control, and lower computer communication subroutine. Among them, the timing subroutine and the lower computer communication subroutine are shown in Figures 7 and 8.

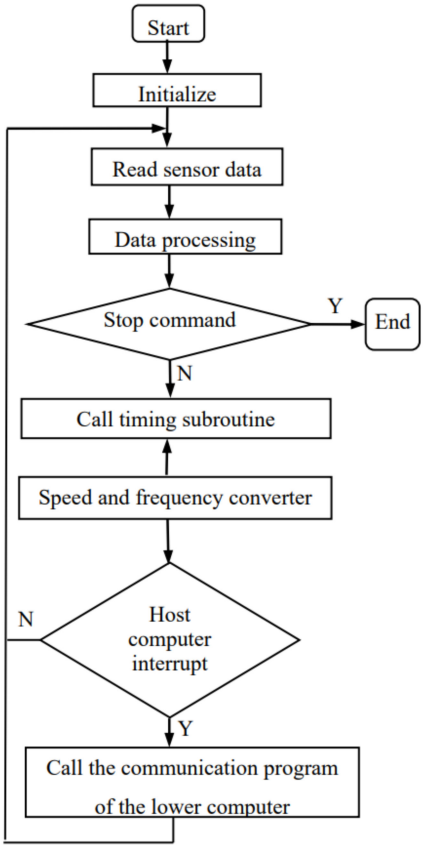

Figure 7. Flow chart of the main program of the slave machine based on PLC.

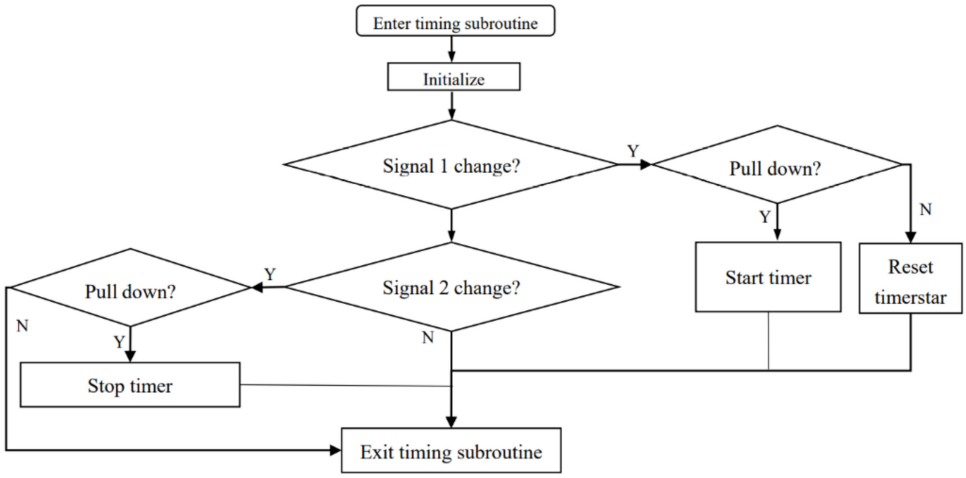

Figure 8. Flow chart of the timing subroutine.

A flow chart showing the design of the timing subroutine is shown in Figure 8. As shown in Figure 8, signal 1 represents the signal change in transmission sensor 1, and signal 2 represents the signal change in transmission sensor 2. When the material enters sensor 1 and covers the receiver, the signal is reduced, and the timer starts to count, waiting for the next command; when the material initially enters sensor 2 and the signal is reduced, the timer stops. At this point, the displayed time is the time required for the material to run the straight-line distance s; when sensor 2's signal is pulled up, it will exit directly; when the signal of sensor 1 is pulled up, the timer is reset.

Finally, in order to ensure the accuracy and reliability of data interaction between the upper and lower computers, MODBUS-RTU protocol is adopted. Based on the Xinjie TG765-

mt touch screen and the xc2-42t PLC core hardware platform, serial port communication compatible with MODBUS-RTU is realized through RS232. The communication between PLC and the actuator through the 485 bus is realized by the same protocol.

An electrical control diagram of the drive motor is shown in Figure 9. It can be seen from Figure 9 that the inverter controls the forward and reverse rotation and speed of the motor, while other switches control the start and stop processes of the motor, and motor 2's control circuit is the same as above. In summary, according to the independent power supply of the cross-cutting tool, the early prototype was improved in two aspects: system mechanism improvement and control system design. The improved prototype is shown in Figure 10.

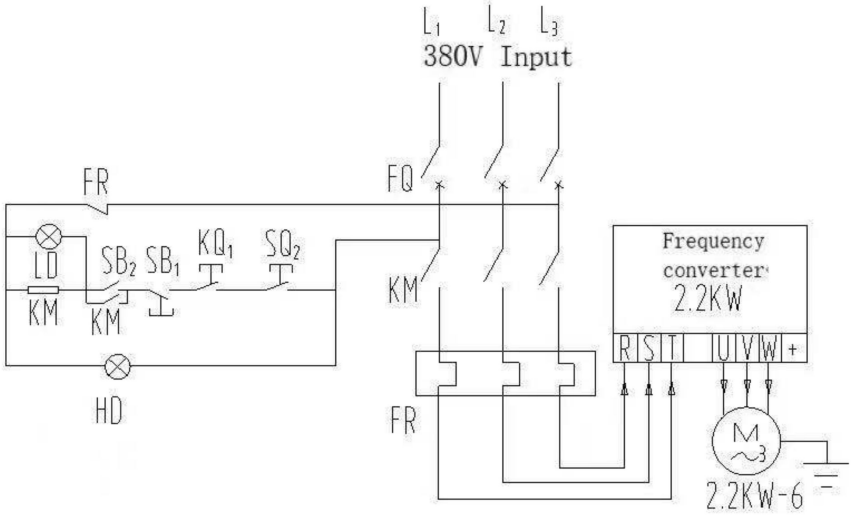

Figure 9. Drive motor's electrical control diagram.

Figure 10. Improved cutting-machine specifications and key components.

3. Experiments and Implementation Details

3.1. Test and Analysis of Specification Cutting Machine before Improvement

Experiments on carrots and potatoes with respect to slicing, strip cutting, and dicing were conducted. The results are shown in Figure 11. The statistical results of the test data are shown in the table below. During the slicing test, the gap between the edge-cutting tool of the roller and the wall of the feeding barrel was set to 11 mm, and the maximum slicing thickness was 11 mm. The speed of the drive motor was 680 r/min, so the speed of the propeller was 194 r/min. Under these conditions, the statistical output results of carrots and potatoes are shown in the table below.

Figure 11. Slicing, strip-cutting, and dicing test chart.

It can be seen from Table 1 that the overall error of carrot slicing is about 19.3% smaller, and that that of potato slicing is about 18.8% smaller.

Table 1. Carrot and potato inspection table. Position.

	Carrot					Potato				
	Position 1	**Position 2**	**Position 3**	**The Average Thickness (mm)**	**Error Rate %**	**Position 1**	**Position 2**	**Position 3**	**The Average Thickness (mm)**	**Error Rate %**
1	8.6	8.9	9.2	8.9	19	8.7	9.2	8.5	8.8	20
2	9.2	9.4	8.4	9.0	18	8.1	8.7	9.1	8.6	22
3	8.6	8.3	9.0	8.6	22	8.9	9.4	8.1	8.8	20
4	8.6	9.4	8.5	8.8	20	8.5	9.2	9.8	9.2	16
5	8.8	9.2	8.5	8.8	20	8.1	9.2	8.4	8.6	22
6	9.1	9.6	8.8	9.2	16	9.7	9.4	9.8	9.6	13
Average thickness (mm)				8.88					8.93	
Average Error %				−19.3					−18.8	

In the combined test implementing slicing and strip cutting, the gap between the edge-cutting tool of the roller and the wall of the feeding barrel was set to 11 mm, the maximum slice thickness was 11 mm, and the disc cutter was set to 10 mm. The speed of the drive motor was 680 r/min, so the speed of the propeller and the disc tool was 194 r/min and 777 r/min, respectively. In this case, the statistical output results are shown in the table below.

It can be seen from Table 2 that the comprehensive error of carrot slicing is 14.9% smaller and that the error of strip cutting is 1.7% smaller. The comprehensive error of potato slicing is 18.5% smaller, and the comprehensive error of strip cutting is 4% smaller. Due to the limitation of the tool gap and the size of the conveying cavity, the size of the material after being sliced and cut into strips is smaller, which is in line with reality.

In the test combining slicing, strip cutting, and dicing, the gap between the edge-cutting tool of the roller and the wall of the feeding barrel was set to 11 mm, the maximum slice thickness was set to 11 mm, the disc cutting tool was set to 10 mm, and the preset size of the cross-cutting tool was 10 mm. The speed of the drive motor was 680 r/min, so the speed of the propeller, disc tool, and cross-cutting tool was 194 r/min, 777 r/min, and 806 r/min, respectively. Under these conditions, the statistics of the carrot and potato output results are shown in the table below.

Table 2. Test table showing combined carrot and potato slicing and strip-cutting results.

	Carrot		Potato	
	Average Slicing Thickness (mm)	**Average Strip-Cutting Thickness (mm)**	**Average Slicing Thickness (mm)**	**Average Strip-Cutting Thickness (mm)**
1	8.9	9.8	8.7	9.7
2	9.2	10	8.9	9.7
3	8.9	10	8.6	9.6
4	9.7	9.6	8.6	9.2
5	9.6	10	9.1	9.4
6	9.6	9.9	8.7	9.6
7	9.6	9.5	10.1	10.0
Average thickness (mm)	9.36	9.83	8.96	9.6
Average Error %	−14.9	−1.7	−18.5	−4.0

It can be seen from Table 3 that the carrot slicing thickness is 16.1% smaller, the strip-cutting thickness is 2.6% smaller, and the dicing thickness is 13.4% larger; the potato slicing thickness is 21.1% smaller, the strip-cutting thickness is 3% smaller, and the dicing thickness is 19.3 % larger.

Table 3. Combined carrot and potato slicing, strip-cutting, and dicing test.

	Carrot			Potato		
	Average Thickness of Slicing (mm)	**Average Thickness of Strip Cutting (mm)**	**Average Thickness of Dicing (mm)**	**Average Thickness of Slicing (mm)**	**Average Thickness of Strip Cutting (mm)**	**Average Thickness of Dicing (mm)**
1	8.7	10	12.6	8.7	9.6	12
2	9.5	10	11.9	9.0	9.7	12.3
3	9.2	9.7	11.7	8.8	9.9	12.7
4	8.9	9.3	10.9	8.3	9.6	10.3
5	9.4	9.4	9.8	8.5	9.7	12.6
6	9.3	9.9	12.3	8.9	9.5	12.5
7	9.6	9.9	10.2	8.6	9.9	11.1
Average thickness (mm)	9.23	9.74	11.34	8.68	9.7	11.93
Average Error %	−16.1	−2.6	13.4	−21.1	−3	19.3

The test analysis is shown below.

The slicing analysis will be discussed first. It can be seen from Figure 4 that there is a certain gap between the slicing tool and the other side of the guide plate, which is adjustable. The gap is the set slicing thickness. Under the dual action of the propeller and the inner wall of the roller, relative movements can be observed in the fruits and vegetables as well as in the slices, causing fruits or vegetables separated from the slices and to be discharged along the gap. The inner wall of the cylinder is arc-shaped, while ideal slices are straight lines. The contact position of the propeller and the roller is inconsistent, resulting in the sliced material not being completely parallel on both sides, meaning that the curve may change. On the other hand, the discharge gap is set, and the thickness of the sliced fruits or vegetables is less than or equal to the gap thickness. There is no better solution for the error caused by the above structure, but in order to optimize the work quality, it is necessary to control the rotation speed of the roller, increasing the centrifugal force on fruits

or vegetables to avoid loosening and resulting in greater errors. As shown in Tables 1–3, the combined errors of the carrot and potato slices are −19.3%, −14.9%, and −16.1% and −18.8%, −18.5, and −21.1%, respectively. This relative error rate will gradually decrease as the slice thickness increases, but it cannot be eliminated.

The strip-cutting analysis will be considered next. It can be seen from Figure 4 that the sliced material slides down along the inclined plane through the discharge channel, where the material is subjected to gravity, reverse friction, and the downward friction force of disc cutting tool. During strip cutting, the size comes from the gap distribution of the blades in the disc tool. Therefore, by adjusting the blade gap, the strip-cutting size can be controlled. By analyzing structure and motion law, the systematic error of strip cutting is very small and can be ignored. Therefore, the strip-cutting size is theoretically very close to the disc blade gap. While the size of the both ends of sliced fruits or vegetables is not controllable, affected by the shape of fruits or vegetables, which is an uncontrollable error from fruits or vegetables. The combined error of carrot and potato cutting is −1.7%, −2.6%; −4%, −3%, respectively.

Finally, we will discuss the details of the dicing analysis. According to the analysis of the dicing mechanism of fruits and vegetables in the first section above, the shape of the dicing section is affected by various parameters, such as the feed speed of the fruits vegetables, the speed of the cross-cutting tool, and the shape of the cutting tool. By establishing the curve equation of the dicing section, the curve of the dicing section is symmetrical, and the rotation speed of the cross-cutting tool is determined by combining the rotational speed of the cylinder and the disc cutting tool.

However, through the experiments, it was found that the actual error of the dicing size is relatively large. According to the cross-sectional equation, it was found that the feed speed of the material is equal to the output speed of the sliced material when the actual material is moving at a variable speed, which is caused by the uncontrollable friction coefficient, as the friction coefficient is related to water content and the proportion of the internal components of the material. The test results in Table 3 show that the combined error of carrot and potato dicing is 13.4% and 19.3%, respectively.

In summary, the dicing tool can be individually closed-loop controlled, and related experiments are carried out below.

3.2. Test and Analysis of Improved-Specification Cutting Machine

Using the improved prototype shown in Figure 10, on 3 June 2021, a dicing test was carried out at Jiangsu LiGong Fruit and Vegetable Machinery Co., Ltd.(Wuxi, China) The drive motor 1 was set to drive the slicing and strip-cutting mechanism, and the speed was determined to be 935 r/min. Drive motor 2 was set to drive the cross-cutting tool, and the speed was determined to be 1390 r/min. This test mainly aimed to achieve the 10 mm dicing requirement in the early stage of the experiment. Through the detection of the material-dicing conveyor speed and by displaying the decision value of the drive speed of the cross-cutting tool, the frequency of drive motor 2 was manually adjusted in order to compare the change in the dicing error before and after the prototype was improved. In addition, for 12 mm dicing, the dicing results were compared to those for the above-mentioned 10 mm dicing.

For the dicing test with the cross-cutting tool size preset to 10 mm, based on the test results and preset parameters before the improvement of the prototype, according to the output speed of drive motor 1, 680 r/min, the frequency of motor 1 was set to 36.36 Hz, and according to the output speed of the cross-cutting tool, 806 r/min, the frequency of motor 2 was set to 28.99 Hz. The carrot's movement speed, 0.07 m/s, and the potato's movement speed, 0.0696 m/s, were obtained from the sensor detection results. The frequency of the drive motor was adjusted from 2 to 30 Hz and 31 Hz for carrot and potato, respectively. The detection interface is shown in Figure 12.

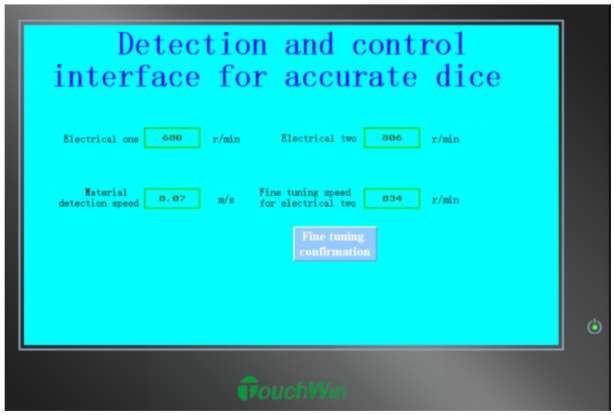

Figure 12. Precise dicing detection and control interface.

It can be seen from Tables 4 and 5 that the error of carrots ranges from −3% to 12%, and the average error is 3.3%; the error of potatoes ranges from 5% to 13%, and the average error is 9%. After fine-tuning motor 2, the average error rate is controlled within 10%.

Table 4. Diced carrot thickness statistics.

Serial Number	Front Dicing (mm)	Center Dicing (mm)	Tail Dicing (mm)	Average Thickness (mm)	Error Rate %	Average Error Rate %
1	10.9	11.0	10.5	10.8	8	3.3
2	9.8	10.5	10.8	10.4	4	
3	9.5	10.8	10.6	10.3	3	
4	10.0	9.8	10.7	10.2	2	
5	9.0	9.4	10.1	9.5	−5	
6	9.8	10.6	10.4	10.3	3	
7	10.7	10.5	10.8	10.7	7	
8	9.8	9.8	10.9	10.2	2	
9	11.2	11.5	10.8	11.2	12	
10	9.8	9.4	9.9	9.7	−3	

Table 5. Diced thickness statistics for potato.

Serial Number	Front Dicing (mm)	Center Dicing (mm)	Tail Dicing (mm)	Average Thickness (mm)	Error Rate %	Average Error Rate %
1	10.7	11.0	10.6	10.8	8	9
2	10.4	10.9	10.3	10.5	5	
3	10.7	11.5	11.2	11.3	13	
4	10.8	11.0	10.5	10.8	8	
5	11.4	11.0	11.2	11.2	12	
6	11.2	11.3	11.0	11.2	12	
7	11.4	10.8	10.8	11	10	
8	10.2	10.5	10.8	10.5	5	
9	10.7	11.0	10.9	10.9	9	
10	10.5	10.9	11.0	10.8	8	

As for the dicing test, where the cross-cutting tool had a preset size of 12 mm, the speed of each tool was set according to the previous theoretical calculations, and the setting principles were consistent with the preset parameters before the improvement of the prototype. The frequency ratio and the rated full scale of drive motor 1 were set to 35.05 Hz and 50 Hz, respectively, so the output speed of motor 1 was 655 r/min, the propeller was set to 187 r/min, and the disc tool was set to 749 r/min; the frequency ratio and the rated full scale of drive motor 2 were set to 25.09 Hz and 50 Hz, respectively, so the actual output speed of drive motor 2 was 697.5 r/min. The size of the toothed-belt output wheel of motor 2 was the same as that of the toothed-belt wheel driven by the power shaft of the cross-cutting tool, so the speed of cross-cutting tool was 697.5 r/min. Under these conditions, the diced thickness statistics for carrot and potato are shown in Tables 6 and 7.

Table 6. Diced thickness statistics for carrot.

Serial Number	Front Dicing (mm)	Center Dicing (mm)	Tail Dicing (mm)	Average Thickness (mm)	Error Rate %	Average Error Rate %
1	13.8	13.0	13.7	13.5	12.5	5.6
2	12.8	12.5	13.4	12.9	7.5	
3	12.5	11.8	12.6	12.3	2.5	
4	13.0	12.8	13.8	13.2	10	
5	11.0	11.4	10.3	10.9	−9.2	
6	12.8	12.4	13.2	12.8	6.7	
7	12.7	12.5	13.5	12.9	7.5	
8	12.8	12.8	13.4	13	8.3	
9	12.2	12.5	12.8	12.5	4.2	
10	12.8	12.4	12.9	12.7	5.8	

Table 7. Diced thickness statistics for potato.

Serial Number	Front Dicing (mm)	Center Dicing (mm)	Tail Dicing (mm)	Average Thickness (mm)	Error Rate %	Average Error Rate %
1	11.7	12.0	11.7	11.8	−1.7	4.5
2	13.4	12.9	13.3	13.2	10	
3	12.7	12.5	13.2	12.8	6.7	
4	11.8	12.0	12.2	12.0	0	
5	12.4	12.0	12.5	12.3	2.5	
6	12.2	12.3	13.0	12.5	4.2	
7	13.4	12.8	12.8	13	8.3	
8	12.2	12.5	12.8	12.5	4.2	
9	12.8	13.0	13.8	13.2	10	
10	12.0	11.9	12.4	12.1	0.8	

According to the analysis of sensor detection data, the average output speed of carrot dicing is 0.0661 m/s, and the average output speed of potato dicing is 0.0672 m/s. The system automatically fine tunes the speed of drive motor 2 during carrot dicing, as the frequency ratio is adjusted to 25.19 r/min, and the actual output speed is 700 r/min. In addition, the system fine tunes the frequency ratio of drive motor 2 during potato dicing to adjust the frequency ratio to 25.29 r/min; the actual output speed of the drive motor 2 is 703 r/min, and the cross-cutting tool is 703 r/min. Under these conditions, the statistics demonstrating the thickness of diced carrot and potato are shown in Tables 8 and 9.

Table 8. Thickness statistics for diced carrot.

Serial Number	Front Dicing (mm)	Center Dicing (mm)	Tail Dicing (mm)	Average Thickness (mm)	Error Rate %	Average Error Rate %
1	12.6	12.2	12.7	12.7	5.8	−0.34
2	11.7	12.2	11.8	12.4	3.3	
3	11.0	11.5	11.4	11.9	−0.8	
4	11.9	12.0	12.7	12.1	0.8	
5	11.8	12.3	11.6	12.5	4.2	
6	10.5	11.2	10.7	11.4	−5	
7	10.8	11.4	10.5	11.5	−4.2	
8	11.7	12.0	12.3	12.0	0	
9	11.0	11.8	10.8	11.4	−5	
10	11.2	11.7	11.6	11.7	−2.5	

Table 9. Thickness statistics for diced potato.

Serial Number	Front Dicing (mm)	Center Dicing (mm)	Tail Dicing (mm)	Average Thickness (mm)	Error Rate %	Average Error Rate %
1	10.8	11.5	11.3	11.2	−6.7	2.1
2	12.1	12.4	13.6	12.7	5.8	
3	11.8	12.4	13.0	12.4	3.3	
4	12.0	12.5	13.6	12.7	5.8	
5	12.6	12.2	12.7	12.5	4.2	
6	12.3	12.3	12.9	12.5	4.2	
7	11.4	12.0	11.4	11.6	−3.3	
8	11.9	12.4	13.8	12.7	5.8	
9	12.1	12.2	11.1	11.8	−1.7	
10	12.2	12.5	12.5	12.4	3.3	

For Tables 6 and 7 and for Tables 8 and 9, three groups of average slip value filtering methods were used to obtain the variation trends in the average thickness error of the dicing process. After average filtering, the error data were reduced from 10 groups to 8 groups, as shown in Table 10.

Table 10. Change trends in dicing error before and after fine-tuning the speed of the cross-cutting tool.

Name \ Serial Number	1	2	3	4	5	6	7	8
Error before carrot fine-tuning %	7.5	6.7	1.1	2.5	1.7	7.5	6.7	6.1
Error after carrot fine-tuning %	2.9	1.1	1.4	0	−1.7	−3.1	−3.1	−2.5
Error before potato fine-tuning %	5.0	5.6	3.1	2.2	5.0	5.6	7.5	5.0
Error after potato fine-tuning %	0.8	5.0	4.4	4.7	1.7	2.2	0.3	2.5

From Table 10, the error range of carrots changes from 1.1% to 7.5% before adjustment to −3.1% to 2.9% after adjustment; the error range of potato dicing changes from 2.2% to 7.5% before adjustment to 0.3~5% after adjustment. The experiment found that due to the

different damping coefficients of the two contexts, the damping of carrot is smaller than that of potato, and the overall movement is decelerated. Therefore, the increase in the frequency of carrot dicing is slightly lower than that of potato, which effectively improves the accuracy and stability of dicing. Compared to the dicing error of dicing with the preset size of 10 mm, the dicing error of dicing with the preset size of 12 mm is relatively decreased due to the increase in the base number. However, based on the speed measurements obtained from the system, the dicing size error of both vegetables can be controlled within 10% after fine-tuning the speed of the cross-cutting tool. The comparative error results before and after adjustment can be seen in Table 11.

Table 11. Comparative error results before and after adjustment.

	Fruits	Subjects	Ave. Error
Average error before fine-turning %	carrot	Slicing (11 mm)	−19.3
		Slicing/strip (11 mm)	−14.9/−1.7
		Slicing/strip/dicing (11 mm)	161/−2.6–13.4
	potato	Slicing (11 mm)	−18.8
		Slicing/strip (11 mm)	−18.5/−4
		Slicing/strip/dicing (11 mm)	−21.1/−3/19.3
Average error after fine-turning %	carrot	Dicing (10 mm)	3.3
		Dicing(12 mm)	5.6
		System auto fine-tuning	−0.34
	potato	Dicing (10 mm)	9
		Dicing (12 mm)	4.5
		System auto fine-tuning	2.1

4. Discussion and Conclusions

In view of the unstable features of material-cutting accuracy, an independent control plan for material-cutting speed detection and for cutting drive is proposed. A material-cutting speed detection system and an independent driving system for a cross-cutting tool is put forward, and technical equipment for accurate control during the three-dimensional cutting of fruits and vegetables is developed.

Before the prototype was improved, the preset slicing requirement was 11 mm under the same conditions, and the slicing errors of carrots and potatoes were limited by the system structure. The slicing errors of carrots and potatoes were −19.3%, −14.9%, and −16.1% and −18.8%, −18.5%, and −21.1%, respectively. The relative error decreased with the increase in slice thickness, but it could not be eliminated. The preset cutting requirement was 10 mm, and the cutting errors of carrot and potato were −1.7% and −2.6%, and −4% and −3%, respectively, and were limited by structure, leading to a smaller size; however, the error rate was acceptable. The preset cutting size was 10 mm, and the cutting errors of carrot and potato were 13.4% and 19.3%, respectively. Carrots have less of a damping effect than potatoes, so the whole material moves at a decreasing speed.

A cutting performance test was implemented using the improved prototype, with the aim of achieving the cutting requirement of 10 mm under the experimental conditions before the improvement. The experimental results show that the error range of carrot is −3~12%, and the average error is 3.3%. The error range of potato is 5~13%, with an average error of 9%. The average error was controlled within 10% after fine-tuning with motor 2. According to the 12 mm cutting requirement, the preset output speeds of motor 1 and motor 2 are 655 rpm and 697.5 rpm, respectively. The cutting speeds of carrot and potato detected by the system were 0.0661 m/s and 0.0672 m/s, respectively, and the precision-adjustment calculations for the speed of motor 2 resulted in 700 r/min and 703 r/min, respectively, so

the carrot error changed from 1.1% to 1.1% before adjustment, and the diced potato error changed from 2.2% to 7.5% before adjustment to 0.3~5% after adjustment. Compared to the preset cutting error of 10 mm, the preset cutting error of 12 mm was relatively reduced due to the increase in the cardinal numbers. However, after measuring the speed of the system, fine-tuning the speed of the cross-cutting tool can ensure that the dimensional error of cutting is controlled within 10%.

Generally speaking, based on traditional three-dimensional fresh-cutting machines, apart from the analysis of force and motion equations to determine the minimum rotational speed of the roller, a cross-cutting tool independent from the drive system, the material required before the implementation of dicing speed detection system, and shaft-speed monitoring have been implemented in this paper in detail to develop precise dicing control. Contrast experiments were carried out on the prototype before and after improvements. The overall dicing error shows great improvement (from 15% down to 10%) as well as improved performance in other areas (such as accuracy and stability).

This research is applicable to other food processing equipment with millimeter precision. In the near future, we want to introduce infrared velocity measurement technology to achieve micron-level machine-accuracy control. Future develops will guarantee velocity measurement and high-speed data processing technology.

Author Contributions: Conceptualization, S.M.; data curation, Z.S. and F.P.; format analysis, S.M.; investigation, Z.S.; methodology, S.M.; validation, Z.S. and F.P.; writing—original draft, S.M.; Writing—review and editing, Y.T. All authors have read and agreed to the published version of the manuscript.

Funding: This work was supported by t the National Key Research and Development Program of China (2018YFD0700304), the fruit, vegetable and tea harvesting machinery innovation project of Chinese Academy of Agricultural Sciences, the Yuyao science and technology innovation project (JHNS20210305) and the Changzhou Sci&Tech Program: CJ20210058.

Institutional Review Board Statement: Not applicable.

Informed Consent Statement: Not applicable.

Data Availability Statement: Not applicable.

Conflicts of Interest: The authors declare no conflict of interest.

References

1. Pang, F.S.; Wang, Y.K.; Pang, H.Q.; Lou, L.; Qian, D.; Cai, B.J. Filed Performance and Comprehensive Evaluation on Chewing Cane Varieties. *China Sugar* **2019**, *41*, 37–41. [CrossRef]
2. Ou, Q. Current situation and development of fruit and vegetable processing industry in China. *Agric. Eng. Technol. (Agric. Prod. Processing)* **2009**, *9*, 28–29. [CrossRef]
3. Yang, M.; Moon, J.; Yang, S.; Oh, H.; Lee, S.; Kim, Y.; Jeong, J. Design and Implementation of an Explainable Bidirectional LSTM Model Based on Transition System Approach for Cooperative AI-Workers. *Appl. Sci.* **2022**, *12*, 6390. [CrossRef]
4. Massaro, A. *Electronics in Advanced Research Industries: Industry 4.0 to Industry 5.0 Advances*; John Wiley & Sons: Hoboken, NJ, USA, 2021. [CrossRef]
5. Filipescu, A.; Ionescu, D.; Filipescu, A.; Mincă, E.; Simion, G. Multifunctional Technology of Flexible Manufacturing on a Mechatronics Line with IRM and CAS, Ready for Industry 4.0. *Processes* **2021**, *9*, 864. [CrossRef]
6. Morgan, J.; Halton, M.; Qiao, Y.S.; Breslin, J.G. Industry 4.0 smart reconfigurable manufacturing machines. *J. Manuf. Syst.* **2021**, *59*, 481–506. [CrossRef]
7. Massaro, A.; Cannella, E.; Dipierro, G.; Galiano, A.; D'Andrea, G.; Malito, G. Maintenance and testing protocols in the railway imdustry. *ACTA IMEKO* **2020**, *9*, 4–12. [CrossRef]
8. Hu, J.P.; Jin, H.Q.; Yang, D.Y. Domestic and international development of the fruits and vegetables dicer. *Agric. Equip. Technol.* **2015**, *41*, 12–15.
9. Zhang, Y.Y.; Li, X.F.; Liu, Y.M. Current situation and development of fruit and vegetable processing industry. *Food More* **2016**, *6*, 90.
10. Jia, Y.J. Present situation and development of fruit and vegetable processing technology. *Digit. User* **2018**, *24*, 34.
11. Qin, J. Processing and preservation technology of fresh fruits and vegetables. *Farmers Consult.* **2018**, *13*, 52. Available online: https://t.cnki.net/kcms/detail?v=eWIMO3hap6NY4Ye-TLDFAJirf4_UynoCoL1d53DNC0Nic9vTDDo3HS-j2rx_FZw5SY_JltqTUHv5toHWGQUXGAx7VLscR3UT7byjlPiOvtMdKXUQRCOBzp8jhUcBKoac&uniplatform=NZKPT (accessed on 10 August 2022).

12. Li, M.L.; Fang, D.Y.; Huang, J.M.; Huang, M.L.; Liu, H.H. Processing and preservation technology of fresh fruits and vegetables. *China Food Saf. Mag.* **2015**, *12*, 55. [CrossRef]
13. Chi, M. Discussion on fresh-cut fruit and vegetable processing technology and fresh-keeping technology. *Mod. Food Sci. Technol.* **2020**, *1*, 76–77. [CrossRef]
14. Zhu, H.Q. Development of QP-320 fresh ginger slicer. *Xinjiang Agric. Mech.* **2009**, *3*, 46–47. [CrossRef]
15. Yang, D.Y.; Hu, J.P.; Xu, X.D.; Huang, Y.S. Development of multifunctional fresh cutting machine for fruits and vegetables. *Food Mach.* **2012**, *28*, 183–185. [CrossRef]
16. Yang, P.G.; Liu, L.P.; Xiong, S.H. Design and optimization of a new lotus slicer. *Food Mach.* **2014**, *2*, 99–101. [CrossRef]
17. Jin, H.Q.; Hu, J.P.; Yang, D.Y. Improved simulation model and test of three-dimensional dicing machine for fruits and vegetables. *Food Mach.* **2016**, *32*, 72. [CrossRef]
18. Hu, J.P.; Huang, Y.S.; Yang, D.Y. Design and experiments of the fruit and vegetable three-dimensional dicing machine. *Trans. Chin. Soc. Agric. Eng.* **2011**, *27*, 353–357. [CrossRef]
19. Yang, D.Y.; Hu, J.P.; Xu, X.D.; Huang, Y.S.; Shi, G.H. Optimization design of fruits and vegetables dicing machine. *J. Mach. Des.* **2012**, *29*, 50–53. [CrossRef]
20. Hu, J.P.; Yang, L.H.; Yang, D.Y.; Huang, Y.S. Section shape deviation analysis of fruits and vegetables three-dimensional dicing machine. *Food Mach.* **2015**, *31*, 84–87. [CrossRef]